LOK is a major ERM kinase in resting lymphocytes and regulates cytoskeletal rearrangement through ERM phosphorylation

Natalya V. Belkina[a], Yin Liu[a], Jian-Jiang Hao[a], Hajime Karasuyama[b], and Stephen Shaw[a,1]

[a]Experimental Immunology Branch, National Cancer Institute, National Institutes of Health, Bethesda, MD 20892; and [b]Department of Immune Regulation, Tokyo Medical and Dental University Graduate School, Bunkyo-ku, Tokyo 113-8519, Japan

Edited by Susan S. Taylor, University of California at San Diego, La Jolla, CA, and approved January 28, 2009 (received for review June 19, 2008)

ERM (ezrin-radixin-moesin) proteins mediate linkage of actin cytoskeleton to plasma membrane in many cells. ERM activity is regulated in part by phosphorylation at a C-terminal threonine, but the identity of ERM kinases is unknown in lymphocytes and incompletely defined in other mammalian cells. Our studies show that lymphocyte-oriented kinase (LOK) is an ERM kinase in vitro and in vivo. Mass spectrometric analysis indicates LOK is abundant at the lymphocyte plasma membrane and immunofluorescence studies show LOK enrichment at the plasma membrane near ERM. In vitro peptide specificity analyses characterize LOK as a basophilic kinase whose optimal substrate sequence resembles the ERM site, including unusual preference for tyrosine at P–2. LOK's activity on moesin peptide and protein was comparable to reported ERM kinases ROCK and PKC but unlike them LOK displayed preferential specificity for moesin compared to traditional basophilic kinase substrates. Two genetic approaches demonstrate a role for LOK in ERM phosphorylation: cell transfection with LOK kinase domain augments ERM phosphorylation and lymphocytes from LOK knockout mice have >50% reduction in ERM phosphorylation. The findings on localization and specificity argue that LOK is a direct ERM kinase. The knockout mice have normal hematopoietic cell development but notably lymphocyte migration and polarization in response to chemokine are enhanced. These functional alterations fit the current understanding of the role of ERM phosphorylation in regulating cortical reorganization. Thus, these studies identify a new ERM kinase of importance in lymphocytes and confirm the role of ERM phosphorylation in regulating cell shape and motility.

ezrin | kinase specificity | knockout | migration | moesin

The ERM family in mammals consists of 3 closely related members: ezrin, radixin and moesin whose major function is to link cortical actin filaments to the plasma membrane (1–4). ERM N terminus (the FERM/band 4.1 domain) binds to plasma membrane both by direct interaction with phospholipids and by binding cytoplasmic tails of transmembrane proteins such as CD43, CD44, and ICAMs. ERM C terminus ("tail") binds to filamentous actin. ERMs exist not only in this active conformation, but also in an inactive conformation where the C terminus binds to the FERM domain, thereby blocking binding sites on both FERM and tail. There is an evolutionarily conserved phosphorylation site near the C terminus whose phosphorylation contributes to stabilizing the active conformation. In mitotic cells ERM phosphorylation is critical for achieving spherical morphology and rigidity (5, 6). For lymphocytes circulating in blood, ERM phosphorylation is understood to contribute to rigidity and maintenance of microvilli. In response to chemotactic factors (especially chemokines) those lymphocytes transition into flexible migrating cells concurrent with rapid extensive dephosphorylation of ERM, which facilitates their polarization (7–10).

Given the importance of ERM phosphorylation, it is essential to identify the kinase(s) that mediate this phosphorylation. Ten years ago the first 2 such candidate ERM kinases reported were PKC-θ (11) and ρ-kinase (12, 13) but controversies remain (14, 15) and since then at least 6 other mammalian kinases have been proposed to be ERM kinases. Most of the work in mammalian cells relates to candidates belonging to the AGC family (e.g., PKC and ROCK) but 2 considerations prompt looking beyond the AGC family for mammalian ERM kinases. First, typical kinases of the AGC family are basophilic kinases that virtually require an arginine residue in at least one critical position before the phosphorylated residue (especially P–3, but also P–2) and benefit from additional positively charged residues nearby (16, 17). In contrast, the ERM phosphorylation site lacks R at either of these positions and has an unusual bulky aromatic residue at P–2. Second, studies in the important model organism Drosophila have implicated a kinase called SLIK, from a very divergent family of kinases, the STE20-related family (STE) (5, 6, 18). More recently one mammalian kinase in the STE family, HGK, was proposed to function as an ERM kinase (19). Thus, mammalian ERM kinases likely include ones outside the AGC family and in the STE family.

The present study identifies lymphocyte-oriented kinase (LOK) as the dominant ERM kinase in hematopoietic cells. It is a little-studied member of the STE family that was identified about 10 years ago and noted to be preferentially expressed in hematopoietic cells but no substrates have been identified (20). LOK−knockout (KO) mice had no gross phenotype, but increased aggregation was observed in cultured Con A-activated lymphocytes (21). We demonstrate LOK to be an ERM kinase on the basis of studies in vitro, *in cells*, and in vivo in the KO mouse. Our studies of peptide specificity reveal it to be basophilic kinase whose unusual features, including a preference for tyrosine at the P–2 position, make it perfectly suited to mediate ERM phosphorylation. Increased efficiency of migration observed in LOK KO lymphocytes is consistent with relaxation of cortical cytoskeleton resulting from reduced levels of ERM phosphorylation.

Results

LOK Is Enriched in Lymphocyte Plasma Membrane and Colocalized with cpERM. ERM phosphorylated on the site near its C terminus (cpERM) is enriched at the lymphocyte plasma membrane (7) and it is plausible, therefore, that the kinase that phosphorylates it is also enriched at the plasma membrane. To identify such a kinase, we mined data from mass spectrometric analysis of proteins in a membrane-microvillus fraction (MMV) of human

Author contributions: N.V.B., Y.L., J.-J.H., and S.S. designed research; N.V.B., Y.L., and J.-J.H. performed research; H.K. contributed new reagents/analytic tools; N.V.B., Y.L., J.-J.H., and S.S. analyzed data; and N.V.B. and S.S. wrote the paper.

The authors declare no conflict of interest.

This article is a PNAS Direct Submission.

[1]To whom correspondence should be addressed. E-mail: sshaw@nih.gov.

This article contains supporting information online at www.pnas.org/cgi/content/full/0805963106/DCSupplemental.

CELL BIOLOGY

A

KINASE	# PEPTIDE	
	MMV	PNL
LOK	13	3
DCAMKL3	2	4
TITIN	3	1
MST2	1	3
p90-RSK2	1	2
MST1	1	2
ROCK-1	1	1
PRK1	0	2
HUNK	0	2
TOTAL PEPTIDES	3596	6676

B

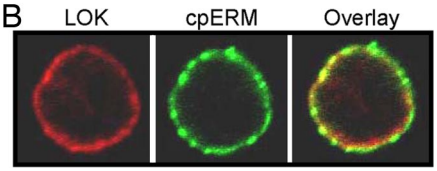

Fig. 1. LOK is abundant at the lymphocyte plasma membrane and colocalized with cpERM. (*A*) Tabulation of kinase peptides detected in mass spectrometric analysis of fractions from human lymphocytes. Fractions: MMV, membrane/microvillus; PNL, postnuclear lysate. (*B*) Colocalization of cpERM (green) and LOK (red) at human lymphocyte plasma membrane detected by immunofluorescence.

lymphocytes (22). The relative abundance of any given protein can be crudely estimated by the number of its identified peptides. In this study 9 kinases were identified by the conservative criterion of detecting 2 or more of its unique peptides (Fig. 1*A*). The mass spectrometric data suggested that LOK is an abundant kinase at the plasma membrane, where it is apparently enriched severalfold relative to postnuclear lysate. Immunofluorescent confocal microscopy confirmed that LOK protein localized to the plasma membrane in close proximity to cpERM (Fig. 1*B*).

LOK Has Strong Specificity for ERM both at the Peptide and Protein Levels. We investigated the peptide and protein specificity of LOK to explore the possibility that LOK has suitable substrate specificity to be an ERM kinase. Analysis of the distribution of negatively charged residues in the substrate binding cleft of LOK suggested that it was likely to be a basophilic kinase (Fig. S1). Therefore our initial analysis characterized LOK's capacity to phosphorylate a panel of 90 peptides from the human proteome that had been chosen as candidate substrates for basophilic kinases by virtue of having 3–5 basic residues near the S/T residue. Surprisingly, only about 10% of the peptides were well phosphorylated, which is a distinctly lower frequency than for PKC and ROCK (Fig. S2). Moreover, LOK's specificity, as assessed by this panel is divergent from that of ROK and PKC (Fig. S2).

To achieve a more detailed understanding of peptide specificity of LOK, we compared it to ROCK (one of the best characterized ERM kinases) using a powerful degenerate peptide library approach developed by Turk et al. (23). The method evaluates which amino acids are favored or disfavored by the kinase in positions near the phosphorylation site. ROCK's most prominent characteristics are those of a basophilic kinase, namely a preference for basic residues near the phosphorylation site, especially N-terminal to it (Fig. 2 *A* and *B*). This preference is also shared by PKC-θ, another candidate ERM kinase (11, 23, 24). LOK too has a preference for basic residues, but the most prominent feature of LOK's peptide specificity is its strong and unusual preference for Y at P–2 (2 amino acids before the phosphorylation site), which is not shared by ROCK (Fig. 2 *A* and *B*) or other classic basophilic kinases tested (23, 24). Note that the ERM phosphorylation site has a Y at exactly that position (Fig. 2*C*), which is absolutely conserved among ERM proteins from worms to human.

Assessment of specificity of LOK, ROCK, and PKC was extended by kinetic analysis both on native moesin peptide and a peptide in which the Y at P–2 was substituted by R. LOK's activity (k_{cat}) was comparable to ROCK and PKC on moesin peptide (Fig. 2*D*, Fig. S3). But marked differences in specificity were highlighted by comparison of native peptide to the Y556R

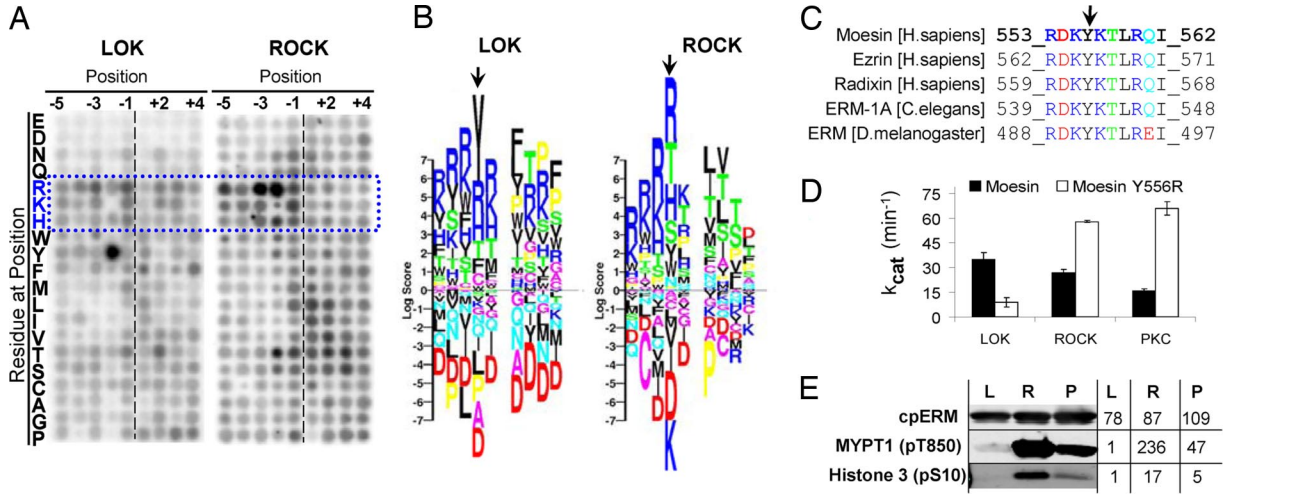

Fig. 2. LOK has distinctive specificity for the ERM C-terminal phosphorylation site. (*A*) In vitro phosphorylation in solution of a degenerate peptide set (24) by LOK and ROCK. The intensity of each spot represents the amount of ^{32}P incorporated into the corresponding degenerate peptide and therefore the kinase's preference for the particular residue at the indicated substrate position. Blue dotted frame and letters indicate basic amino acids. (*B*) The results from panel *A* are represented as a PSSM logo (25). Each stack of letters represents the kinase's preference for each possible residue at a single substrate position around the phosphorylation site (P0). Positions before P0 are represented as P minus (P–1, P–2) and after as P plus (P+1, P+2). The height of each letter is proportional to the absolute value of the log score of that preference and the positions of the letters in the stack are sorted from *Bottom* to *Top* in ascending value by the log score. Thus, strongly favored residues are at the *Top* and strongly disfavored residues are at the *Bottom*. Color indicates physicochemical properties of which the most relevant here are blue for basic, red for acidic, and black for hydrophobic. Arrow indicates P–2 position. (*C*) Sequences of the phosphorylation site in ERM from human, worm, and insect. Phosphorylation occurs on T and arrow indicates conserved Y at P–2. (*D*) Kinetic analysis of in vitro phosphorylation by LOK, ROCK, and PKC-θ of 2 peptides: WT moesin and mutant peptide where Y at P–2 is substituted with R (see also Fig. S3). (*E*) Phosphorylation of individual sites on 3 proteins by LOK (L), ROCK (R), and PKC-θ (P). Phosphorylated sites detected are: T558 on moesin C terminus (302–577), S10 on histone H3, and T850 on MYPT1 (654–880). Numbers to the *Right* of blots indicate level of fluorescent emissions from corresponding bands.

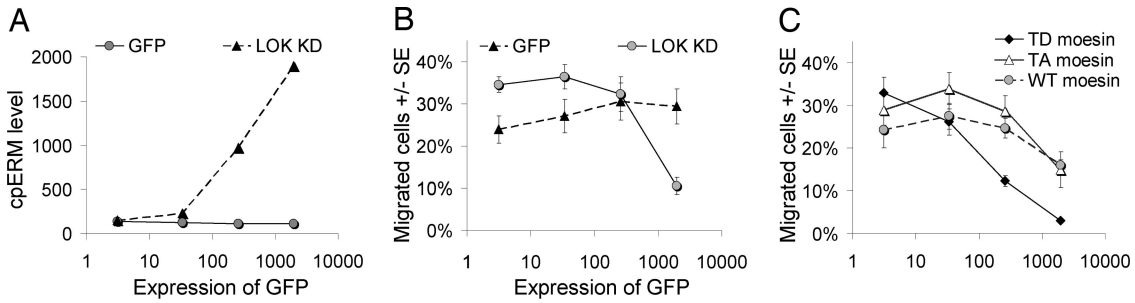

Fig. 3. Evidence in Jurkat cells that LOK phosphorylates ERM and that ERM phosphorylation impedes migration. (*A*) Jurkat cells were transfected with LOK KD or GFP control and cpERM was detected by flow cytometry after 18 h. Cells from each preparation were separated into 4 categories by absolute GFP fluorescence i.e., nontransfected (0–10), low level expression (10–100), medium level expression (100–1000), and high level expression (>1000). (*B*) Same transfected cells as panel *A* analyzed for transmigration in response to SDF-1. (*C*) Jurkat cells were transfected with pseudophosphorylated (T558D), nonphosphorylated (T558A), or WT moesin GFP fusion protein and analyzed for transmigration in response to SDF-1.

peptide. LOK had much higher activity (≈4 times) on the native sequence, confirming LOK's strong preference for Y at P–2; in contrast, PKC and ROCK had the opposite preference for the mutated sequence (≈4 and ≈2 times, respectively), confirming their conventional basophilic preference for R at P–2.

Since *peptide* phosphorylation is only partially predictive of protein phosphorylation, *protein* specificity was also assessed. A first round of analysis of specificity was conducted by measuring the activity of LOK, PKC, and ROCK on ERM, and a histone fraction and MYPT1 (classical basophilic substrates for PKC and ROCK, respectively) by ^{32}P incorporation (Fig. S4). All 3 kinases mediated the same order of magnitude of phosphorylation of ERM. But despite the availability of many potential basophilic phosphorylation sites on MYPT1 and the histone fraction, LOK's phosphorylation was virtually restricted to ERM, while ROCK and PKC phosphorylated both the other substrates as much or more than they phosphorylated ERM. To assess phosphorylation of the single relevant site on ERM, phospho-specific antibody was used for detection in immunoblots and the results compared to single sites on histone H3 and MYPT1 (Fig. 2*E*). The results confirm that LOK, ROCK, and PKC do not differ enormously in their phosphorylation of ERM, but LOK does not efficiently phosphorylate the other 2 basophilic sites assessed.

Evidence in Jurkat Cells That LOK Phosphorylates ERM and That ERM Phosphorylation Impedes Migration. To assess the role of LOK as an ERM kinase in cells, we overexpressed GFP-tagged LOK kinase domain (KD) in Jurkat cells. LOK transfected cells have increased ERM phosphorylation and the level of cpERM increases as the amount of transfected LOK KD increases (Fig. 3*A*). On the basis of previous functional studies of ERM activation we anticipated that cells having increased ERM phosphorylation would have decreased lymphocyte mobility, measured in a transmigration assay, which involves polarization, migration, and deformation through a membrane pore in response to chemokine. This prediction was confirmed by impairment of migration at the highest levels of LOK transfection (Fig. 3*B*). To test whether ERM-hyperphosphorylation per se can mediate such migration inhibition, we exploited transfection with pseudophosphorylated (T558D), nonphosphorylated (T558A), and WT moesin GFP fusion constructs. As predicted, pseudophosphorylated moesin was the most efficient in inhibiting migration (Fig. 3*C*).

Lymphocytes from LOK KO Mice Have Decreased ERM Phosphorylation and Respond Better to Chemokine Stimulation in Chemotaxis and Polarization. LOK KO mice (21) provide a powerful genetic model to test the hypothesis that LOK is a major ERM kinase. Since LOK is primarily expressed in hematopoietic cells (20) we investigated ERM phosphorylation in lymphocytes. Western blot (WB) analysis showed that cpERM in LOK KO mice (*lok*–/–) was markedly reduced relative to heterozygote littermates (*lok*+/–) in lymph node, spleen, and bone marrow cells (Fig. 4*A*). Levels of expressed moesin and ezrin were indistinguishable (data not shown). Quantitative analysis indicated ≈4-fold reduction in cpERM in the KO (Fig. 4*B*). Immune system development appeared normal in the KO mouse, in keeping with the initial report (21). Notably, although cpERM is enriched in normal lymphocyte microvilli, SEM analysis revealed little or no reduction in lymphocyte microvilli from LOK KO mice (Fig. 4*C*).

We extended the analysis of LOK KO lymphocytes by studying in vitro lymphocyte transmigration in response to a chemotactic stimulus. LOK KO cells transmigrated more effectively than heterozygous littermate controls (Fig. 5*A*). Thus, migration was facilitated in these cells having decreased cpERM, and conversely migration was impaired in Jurkat cells whose ERM

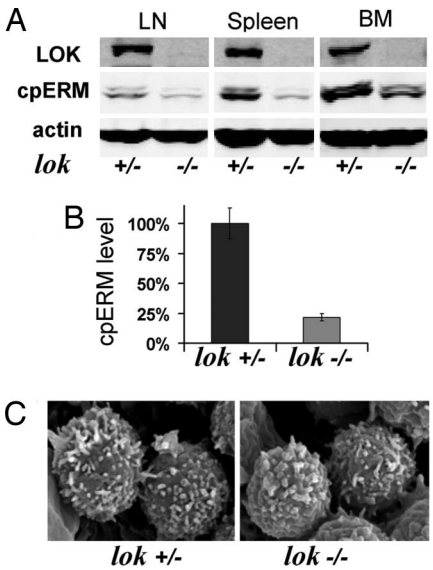

Fig. 4. Hematopoietic cells from LOK KO mice have decreased ERM phosphorylation without major change in lymphocyte microvilli. (*A*) Example of WB detection of cpERM, and actin in lysates from hematopoietic cells from different tissues, LN, lymph nodes; BM, bone marrow. (*B*) Comparison of cpERM level in spleen cells from 10 pairs of LOK KO mice and their heterozygote littermates. (*C*) SEM images of lymph node lymphocytes from a LOK KO mouse and its littermate.

CELL BIOLOGY

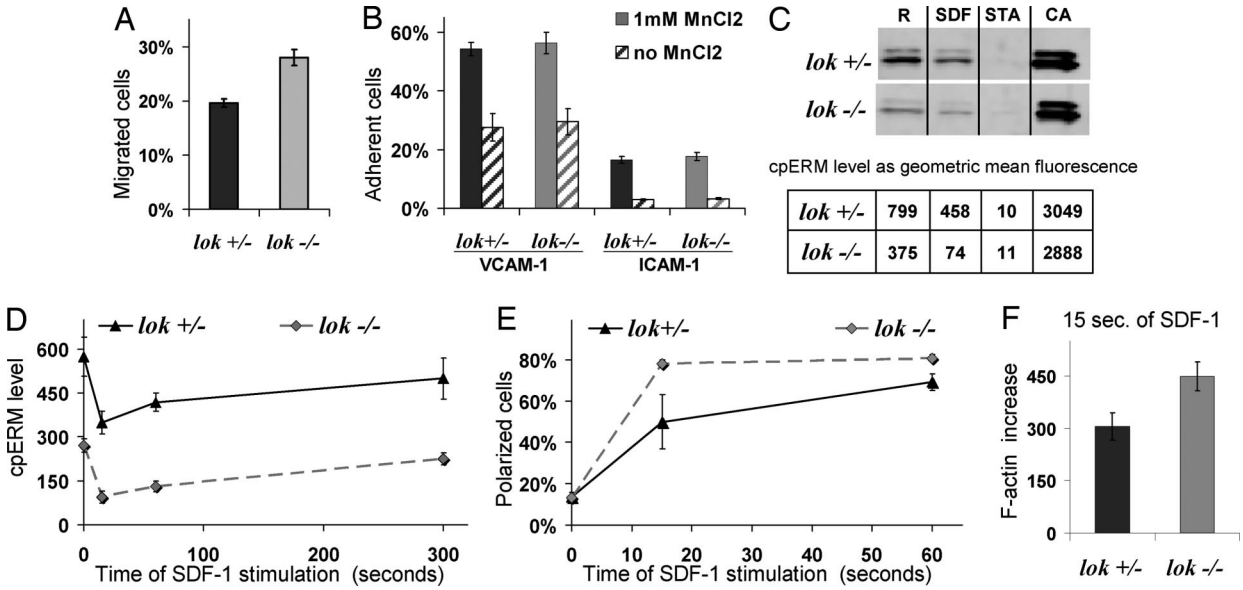

Fig. 5. LOK depletion results in alteration of migration and polarization, but not in adhesion. (*A*) Splenic lymphocytes from LOK KO mice and littermate controls were analyzed for transmigration to SDF-1. (*B*) Splenic lymphocytes from LOK KO mice and littermate controls were analyzed for adhesion to VCAM-1 or ICAM-1. Assays were performed in the presence or absence of 1 mM $MnCl_2$, which promotes conversion of integrins into active conformation. (*C*) Splenic lymphocytes from LOK KO mice and littermate controls were analyzed for cpERM phosphorylation under 4 standard conditions: R, resting, no treatment; SDF-1, 1 min after 100 ng/mL SDF-1 to assess physiological dephosphorylation; STA, 5 min after high concentration (500 nM) staurosporine to assess maximal dephosphorylation; CA, 5 min after 50 μM phosphatase inhibitor calyculin A to maximize phosphorylation; cpERM was assessed both by WB (*Upper* subpanel) and flow cytometry (*Lower* subpanel). (*D*) cpERM levels were measured for splenic lymphocytes from LOK KO mice and littermate controls before and after various times of stimulation with SDF-1. (*E*) Cells as in panel *D*, but stained with phalloidin to detect F-actin and scored blind for polarization. (*F*) Cells as in panel *E*, but analyzed for increase in F-actin by flow cytometry after 15 s of stimulation.

phosphorylation was increased by LOK transfection (Fig. 4*B*). Adhesion assays provided no evidence of altered adhesion that would explain migration differences (Fig. 5*B*). Flow cytometry provided quantitative single cell analysis of ERM phosphorylation, whose pattern was validated by comparison with WB results (Fig. 5*C* and Fig. S5). It is important to explore cpERM level not only in unstimulated cells, but also during the chemokine response (Fig. 5*D*). Reduction of cpERM after SDF-1 stimulation was greatest at 15 s, at which time 30−50% of cpERM remained (Fig. 5 *C* and *D*). Thereafter the cpERM level gradually increased to the basal level. At every time point studied, cpERM levels were lower in LOK KO than in heterozygotes. Clearly there is a residual ERM kinase(s) in the LOK KO lymphocytes because: (*i*) the maximum phosphorylation of ERM caused by phosphatase inhibitor calyculin A treatment is comparable in KO and littermate cells (Fig. 5*C*), and (*ii*) the progressive cpERM rephosphorylation after SDF-1 stimulation is not dramatically delayed (Fig. 4*D*).

We predicted that the LOK KO lymphocytes would have facilitated polarization in response to chemokine on the basis of previous findings with in vitro transfected cells (7). In LOK KO more lymphocytes polarized after 15 s of SDF-1 stimulation than in heterozygous controls (80% vs. 50%) (Fig. 5*E*). Chemokine stimulation of lymphocytes induced rapid actin polymerization, which contributes to lamellipodium formation. In keeping with the accelerated polarization of KO lymphocytes, their early increase in F-actin was also more pronounced (Fig. 5*F*).

Discussion

Four convergent lines of evidence described herein establish that LOK is a major ERM kinase in lymphocytes. Evidence from the LOK KO mouse provides the single most powerful supporting evidence, because ERM phosphorylation is markedly reduced in such mice. Conversely, transfection of a cell line with LOK augments ERM phosphorylation. The other 2 lines of evidence implicate LOK as an ERM kinase per se rather than as an upstream regulator of an ERM kinase. First, LOK is preferentially found at the plasma membrane, the dominant location of ERM phosphorylation. Second, the ERM phosphorylation site consists of an amino acid sequence that is close to optimal for LOK phosphorylation and includes particularly a Y at the P–2 position distinguishing it from optimal substrates for classic basophilic kinases (which strongly prefer R there). LOK is thus shown to be an ERM kinase by both genetic and biochemical means.

LOK has both major similarities and differences from most reported ERM kinases. First LOK is *not* a member of the AGC family of kinases, unlike, for example, ROCKs and PKCs. On the contrary, LOK is a member of GCK branch of the STE kinase family, which is taxonomically far removed from the AGC family and about which much less is known. But LOK shares one cardinal feature of the best-studied candidate ERM kinases—it is a basophilic kinase. However, because there are many basophilic kinases, other features must confer further specificity; these include specific localization of the kinase and additional features in peptide specificity. Notably, LOK has a strong distinctive preference for a Y at the P–2 position, unlike any other well characterized basophilic kinase. This Y confers a 4-fold increase in preference of LOK for the ERM site (relative to R, which is preferred by prototypic ERM kinases ROK and PKC). Thus, LOK generally resembles the basophilic preference of AGC family kinases (apparently by convergent evolution), but has singular specificity for ERM that is imparted in part by a distinctive preference for Y at P–2.

Multiple emerging lines of evidence suggest that GCK family kinases in addition to LOK play important roles in ERM phosphorylation. HGC was reported to phosphorylate ERM in the lamellipodium of growth factor-stimulated human epithelial cells (19). Drosophila provides a particularly informative model because of its reduced number of kinases and a single ERM

protein. In Drosophila, SLIK kinase is necessary for in-cell phosphorylation of moesin (5, 6, 18). Sequence analysis shows that insect SLIK is the ortholog of a 2-member subfamily of mammalian GCK kinase: LOK and SLK (KD sequence similarity 80% to SLK/LOK but <60% to other kinases). Although the Drosophila studies did not address kinase specificity, our findings complement their data and strongly suggest a direct role for SLIK phosphorylation of ERM in those systems. In addition, human SLK regulates microtubule organization in mitotic cells via its kinase activity (25) in a manner similar to that of Drosophila SLIK (in which the link to ERM phosphorylation was established). Since SLK is widely expressed (26) we hypothesize that SLK in addition to other reported ERM kinases may mediate the ERM phosphorylation that remains in LOK KO lymphocytes.

LOK has a dominant role in ERM phosphorylation in lymphocytes even though other reported ERM kinases (e.g., ROCK and PKC-θ) are expressed in lymphocytes and have comparable catalytic activity on ERM proteins (Fig. 2 and Figs. S3 and S4). An appealing explanation for LOK's dominance is higher local concentration of LOK than other ERM kinases in the vicinity of the plasma membrane, which is suggested by mass spectrometric evidence (Fig. 1*A* and data not shown) and paralleled by immunofluorescence analysis of colocalization with cpERM (Fig. 1*B*). A potential risk arising from high concentration of kinase at the plasma membrane is unintended phosphorylation of other S/T sites. This risk may be minimized by LOK's atypical basophilic specificity, as compared, for example, to ROCK's conventional basophilic specificity. First, LOK's specificity results in a low frequency of phosphorylation of conventional basic substrates (Figs. S3 and S4) compared for example with ROCK. Second, LOK's unusual strong preference for Y at P–2 may minimize problematic crossreactions, because: (*i*) Y is overall ≈2 times less abundant in the proteome than R and (*ii*) analysis of residue frequency at the P–2 position indicates R is markedly overrepresented in identified in vivo phosphorylation sites of mammalian proteins but Y is not (Fig. S6). Other mechanisms may also contribute. For example, docking of LOK to moesin and regulated activation of LOK are important subjects for future investigation whose contribution in our assays may have been limited because of use of a constitutively active kinase domain.

The present studies extend the current view of ERM phosphorylation in lymphocyte polarization and migration in response to chemokine. Efficient migration of primary lymphocytes is understood to require transition from a relatively rigid spherical organization to a relatively flexible motile morphology. Part of this transition involves sequestration into a trailing uropod of rigid elements such as intermediate filaments (27). In addition cortical rigidity is contributed by ERM proteins and especially by phosphorylated ERM proteins (6, 10). Rapid chemokine-induced ERM dephosphorylation would thus also contribute to facilitation of polarization by relaxing the rigidity of the cortical cytoskeleton in resting lymphocytes. As predicted by this model, it has been shown that overexpression of moesin-T558D impairs polarization in lymphocytes (7) and impairs migration in Jurkat cells (Fig. 3*C*). Similarly, overexpression of kinase domain of LOK in Jurkat cells increases ERM phosphorylation and impairs migration (Fig. 3*B*). Conversely in lymphocytes from the LOK KO mouse, cpERM levels are decreased and migration is increased (Figs. 4 and 5). In these studies we chose to investigate uncultured primary cells from the LOK KO to minimize complexities resulting from ex vivo culture. However, the findings by Karasuyama and colleagues on cultured cells (21) can plausibly be explained by changes in cpERM. Less ERM phosphorylation in the cultured KO cells would be expected to result in cortical relaxation and release of cytoplasmic tails of multiple transmembrane molecules. These processes could account for increased lateral mobility of surface molecules, enhanced redistribution of LFA-1 molecules, and enhanced aggregation.

These biochemical studies demonstrate that LOK is an effective ERM kinase with distinctive specificity for the critical phosphorylation site in ERM. LOK functions as the dominant ERM kinase in primary mouse lymphocytes and contributes to regulation of lymphocyte migration apparently via ERM phosphorylation. The relative normalcy of immune development and function in the LOK KO likely reflects multiple levels of failsafe protections. First, an alternative ERM kinase(s) provides at least one-quarter of normal levels of ERM phosphorylation. Second, other mechanisms of ERM activation, probably those mediated by PIP2-induced activation, apparently provide sufficient active ERM to maintain cortical rigidity and stabilize microvilli.

Materials and Methods

General. Human lymphocytes were isolated as described (7) and resuspended in HBSS with 10 mM Hepes and 0.2% BSA. Jurkat-T cells (kindly provided by G. Crabtree, Stanford University) were grown in RPMI1640 (Invitrogen), containing L-glutamine and 25 mM Hepes, with 10% FBS (HyClone). Single-cell suspensions of mouse spleen, lymph node, and bone marrow were prepared in RPMI1640 with 0.2% BSA and 50 μM of β-mercaptoethanol. Cells were placed in polystyrene round-bottom tubes or in polypropylene microcentrifuge tubes at 5–20 $\times$ 10^6/mL and warmed to 37 °C on a rocking platform for at least 1 h before use. SDF-1 chemokine was purchased from PeproTech. The following antibodies were used: carboxy-terminal LOK rabbit pAb (Bethyl), β-actin mouse mAb (Sigma-Aldrich), cpERM mouse mAb from BD Biosciences. cpERM mAb was conjugated with AlexaFluor647 (Invitrogen). AlexaFluor488 phalloidin, ROCK2 human kinase, and 2′,7′-bis-(2-carboxyethyl)-5-(and-6)-carboxyfluorescein acetoxymethyl ester (BCECF) were purchased from Invitrogen. Human PKC-θ and LOK kinase domain (1–348) tagged at its N terminus with hexahistidine were expressed in baculovirus and purified by nickel affinity chromatography. SDS/PAGE and silver staining were carried out to verify the purity. Moesin (302–577) was expressed and purified as GST fusion proteins according to GST Gene Fusion System Handbook (Amersham Biosciences). The degenerate peptide library (24) was a generous gift from B. Turk (Yale University), moesin WT and mutated peptides were synthesized by Peptron Inc. Histone (≈subgroup f1) was from Sigma-Aldrich, MYPT1 (654–880), phospho-MYPT1 (Thr-850) rabbit mAb, human histone H3, phospho-histone H3 (Ser-10) mouse mAb and calyculin A were from Millipore. Staurosporine was obtained from EMD, [γ-^{32}P]ATP was from GE Healthcare. Mouse recombinant ICAM-1 VCAM-1 proteins were purchased from R&D Systems. LOK KO mice have been previously described (22). Animal protocols were approved by the NCI Animal Care and Use Committee. All experiments were done at least 3 times with similar results.

Cell Transfection, Adhesion and Migration Assay. Expression vectors (pMSCV IRES GFP) for moesin WT, T558A, and T558D were a kind gift from J. Delon (Institut Cochin, Paris, France). LOK KD vector (pEGFP-N3) was a gift from A. Avery (Pennsylvania State University). Empty vector pmaxGFP was purchased from Amaxa. Cells were transfected by electroporation with 10 μg of plasmid per 10 $\times$ 10^6 cells as described (28). Adhesion of mouse splenic cells to immobilized mouse ICAM-1, VCAM-1, or BSA as a control was performed as previously described (29, 30). Briefly, 96-wells microplates were coated with ICAM-1 or VCAM-1, each well by 50 μL of 10 μg/mL solution, and blocked with 2% BSA. Fluorescence (BCECF)−labeled mouse spleenocytes were washed 3 times in serum-free medium (HBSS with 10 mM Hepes and 0.1% BSA) and resuspended in adhesion media (150 mM NaCl, 10 mM Hepes, 0.1% BSA, 1 mM $CaCl_2$, 1 mM $MgCl_2$, and with or without 1 mM $MnCl_2$) and plated onto the precoated wells (10^5/well) at 37 °C for 30 min. Following the incubation period, the wells were washed 3 times and adhesion was quantified using a fluorescence microplate reader (BIO-TEK). Migration assay was performed by using a Transwell system of polycarbonate membrane with 3-μm pores for primary cells and 5-μm pores for (larger) Jurkat cells (Corning). Cells (2–10 $\times$ 10^6) were put in the upper chamber of transwell; the lower chamber was filled with RPMI1640 with 400 ng/mL SDF-1 and 0.2% BSA. After 2 h, cells were collected and counted using fluorescent beads as a standard (CALTAG/Invitrogen) on a FACSCalibur (BD Biosciences).

Western Blot and Mass Spectrometry. Whole cell lysates were generated as described previously (7). Equal sample volumes were resolved by Novex 4−20% Tris-Glycine PAGE and analyzed by using Odyssey WB Detection

System with Infrared fluorescence (LI-COR Biosciences). Preparation of cellular fractions and LC/MS/MS was previously described (22).

Immunofluorescence, Flow Cytometry and Microscopy. Previously described protocol was used for lymphocyte immunofluorescent staining (7). Murine and Jurkat cells were fixed in suspension by 2% paraformaldehyde for 10 min at 37 °C and then permeabilized BD Perm/Wash Buffer [15 min at room temperature (RT)]. Cells were then washed and stained with fluorescein-conjugated antibody and/or phalloidin for 1 h at RT or overnight at 4 °C followed by 3 washes with BD Perm/Wash Buffer. Cells were analyzed for fluorescence intensity (geometrical mean) on a FACSCalibur. For microscopy, cells were allowed to settle on glass-bottom culture dishes no. 1.5 (MatTek) for 10 min. Single-plane images were collected at the midplane of the cell with a Zeiss LSM 510 META confocal microscope using a 100× (N.A. 1.4) oil-immersion objective lens. Polarization was scored blind (7). For scanning electron microscopy, cells were fixed, processed, observed, and photographed with the S3000N scanning electron microscope (Hitachi) operated at 10 kV as previously described (7).

In Vitro Kinase Assay. Pilot studies were performed to choose assay conditions in which phosphorylation was linear with respect to time and enzyme concentration. Peptides were phosphorylated by an in vitro kinase assay as previously described (23, 24, 31). Briefly peptides as 40 μM of degenerate peptide library were incubated with 18 ng of kinase of interest in the presence of 1 μCi of [γ-^{32}P]ATP in total 16 μL of customized kinase buffer for 30 min at 30 °C. After reaction termination, 2 μL of reaction mix were transferred to streptavidin-coated membrane by using MultiBlot replicator VP382 (V&P Scientific), then the membrane was washed 9 times and exposed to phosphor screen (Amersham) overnight at RT. Reading was done by Storm 860 Molecular Imager (GE Healthcare) and data from digital image were analyzed by TotalLab (Nonlinear Dynamics). For determination of K_m and k_{cat} serial 1.25-fold dilutions of substrate peptides from 12.5 μM to 1.07 μM were used and the assays were performed with 10 nM kinase of interest in the presence of 1 μCi of [γ-^{32}P]ATP in total 50 μL of customized buffer at 30 °C for 10 min. After reaction termination 50 pmol of substrate was transferred to streptavidin-coated plates, and emissions counted after extensive washing by Micro Beta TriLux counter (Perkin−Elmer). K_m and k_{cat} were calculated by GraphPad Prism. Protein phosphorylation was done generally in the same way, except no γ-^{32}P was used. Assays were performed with 20 μM of protein substrate and 60 nM kinase of interest in total 50 μL volume for 30 min at 30 °C. Reaction was stopped by adding 2× reducing SDS sample buffer and samples were separated as described for WB. The gel then was immunoblotted for individual phosphorylation sites. For LOK and ROCK the kinase buffer contained 60 mM Hepes, 10 mM MgCl2, 1 mM NaVO4, 1 mM of DTT, 100 μM of cold ATP, and 0.5 mM EDTA and for PKC-θ differences were 100 mM Hepes, no EDTA, 1 mM CaCl2, 100 ng/mL PMA and 0.2 mg/mL phosphatidylserine (Avanti).

ACKNOWLEDGMENTS. We thank A. Avery, T. Chavakis, G. Crabtree, J. Delon, D. Esposito, W. Gillette, J. Hartley, C. Khanna, M. Kruhlak, K. Nagashima, R. Nijhara, L. Ren, B. Turk, and G. Zhu for sharing of reagents, technical assistance and/or helpful discussion. This research was supported by the Intramural Research Program of the National Institutes of Health, and Center for Cancer Research, National Cancer Institute.

1. Charrin S, Alcover A (2006) Role of ERM (ezrin-radixin-moesin) proteins in T lymphocyte polarization, immune synapse formation and in T cell receptor-mediated signaling. *Front Biosci* 11:1987–1997.
2. Niggli V, Rossy J (2008) Ezrin/radixin/moesin: Versatile controllers of signaling molecules and of the cortical cytoskeleton. *Int J Biochem Cell Biol* 40:344–349.
3. Burkhardt JK, Carrizosa E, Shaffer MH (2008) The actin cytoskeleton in T cell activation. *Annu Rev Immunol* 26:233–259.
4. Bretscher A, Edwards K, Fehon RG (2002) ERM proteins and merlin: Integrators at the cell cortex. *Nat Rev Mol Cell Biol* 3:586–599.
5. Carreno S, et al. (2008) Moesin and its activating kinase Slik are required for cortical stability and microtubule organization in mitotic cells. *J Cell Biol* 180:739–746.
6. Kunda P, Pelling AE, Liu T, Baum B (2008) Moesin controls cortical rigidity, cell rounding, and spindle morphogenesis during mitosis. *Curr Biol* 18:91–101.
7. Brown MJ, et al. (2003) Chemokine stimulation of human peripheral blood T lymphocytes induces rapid dephosphorylation of ERM proteins, which facilitates loss of microvilli and polarization. *Blood* 102:3890–3899.
8. Nijhara R, et al. (2004) Rac1 mediates collapse of microvilli on chemokine-activated T lymphocytes. *J Immunol* 173:4985–4993.
9. Lee JH, et al. (2004) Roles of p-ERM and Rho-ROCK signaling in lymphocyte polarity and uropod formation. *J Cell Biol* 167:327–337.
10. Faure S, et al. (2004) ERM proteins regulate cytoskeleton relaxation promoting T cell-APC conjugation. *Nat Immunol* 5:272–279.
11. Pietromonaco SF, Simons PC, Altman A, Elias L (1998) Protein kinase C-theta phosphorylation of moesin in the actin-binding sequence. *J Biol Chem* 273:7594–7603.
12. Matsui T, et al. (1998) Rho-kinase phosphorylates COOH-terminal threonines of ezrin/radixin/moesin (ERM) proteins and regulates their head-to-tail association. *J Cell Biol* 140:647–657.
13. Oshiro N, Fukata Y, Kaibuchi K (1998) Phosphorylation of moesin by rho-associated kinase (Rho-kinase) plays a crucial role in the formation of microvilli-like structures. *J Biol Chem* 273:34663–34666.
14. Matsui T, Yonemura S, Amano M, Tsukita S, Tsukita S (1999) Activation of ERM proteins in vivo by Rho involves phosphatidyl- inositol 4-phosphate 5-kinase and not ROCK kinases. *Curr Biol* 9:1259–1262.
15. Yokoyama T, Goto H, Izawa I, Mizutani H, Inagaki M (2005) Aurora-B and Rho-kinase/ROCK, the two cleavage furrow kinases, independently regulate the progression of cytokinesis: possible existence of a novel cleavage furrow kinase phosphorylates ezrin/radixin/moesin (ERM). *Genes Cells* 10:127–137.
16. Pinna LA, Ruzzene M (1996) How do protein kinases recognize their substrates? *Biochim Biophys Acta* 1314:191–225.
17. Zhu G, et al. (2005) A single pair of acidic residues in the kinase major groove mediates strong substrate preference for P-2 or P-5 Arginine in the AGC, CAMK and STE kinase families. *J Biol Chem* 280:36372–36379.
18. Hipfner DR, Keller N, Cohen SM (2004) Slik Sterile-20 kinase regulates moesin activity to promote epithelial integrity during tissue growth. *Genes Dev* 18:2243–2248.
19. Baumgartner M, et al. (2006) The Nck-interacting kinase phosphorylates ERM proteins for formation of lamellipodium by growth factors. *Proc Natl Acad Sci USA* 103(36):13391–13396.
20. Kuramochi S, et al. (1997) LOK is a novel mouse STE20-like protein kinase that is expressed predominantly in lymphocytes. *J Biol Chem* 272:22679–22684.
21. Endo J, et al. (2000) Deficiency of a STE20/PAK family kinase LOK leads to the acceleration of LFA-1 clustering and cell adhesion of activated lymphocytes. *FEBS Lett* 468:234–238.
22. Hao JJ, et al. (2008) Enrichment of distinct microfilament-associated and GTP-binding-proteins in membrane/microvilli fractions from lymphoid cells. *J Proteome Res* 7:2911–2927.
23. Hutti JE, et al. (2004) A rapid method for determining protein kinase phosphorylation specificity. *Nat Methods* 1(1):27–29.
24. Fujii K, et al. (2004) Kinase peptide specificity: improved determination and relevance to protein phosphorylation. *Proc Natl Acad Sci USA* 101:13744–13749.
25. Burakov AV, et al. (2008) Ste20-related protein kinase LOSK (SLK) controls microtubule radial array in interphase. *Mol Biol Cell* 19:1952–1961.
26. Itoh S, et al. (1997) Molecular cloning and characterization of a novel putative STE20-like kinase in guinea pigs. *Arch Biochem Biophys* 340(2):201–207.
27. Brown MJ, Hallam JA, Colucci-Guyon E, Shaw S (2001) Rigidity of circulating lymphocytes is primarily conferred by vimentin intermediate filaments. *J Immunol* 166:6640–6646.
28. Liu Y, Kruhlak MJ, Hao JJ, Shaw S (2007) Rapid T cell receptor-mediated SHP-1 S591 phosphorylation regulates SHP-1 cellular localization and phosphatase activity. *J Leukoc Biol* 82:742–751.
29. Kanse SM, Kost C, Wilhelm OG, Andreasen PA, Preissner KT (1996) The urokinase receptor is a major vitronectin-binding protein on endothelial cells. *Exp Cell Res* 224:344–353.
30. Chavakis T, May AE, Preissner KT, Kanse SM (1999) Molecular mechanisms of zinc-dependent leukocyte adhesion involving the urokinase receptor and beta2-integrins. *Blood* 93:2976–2983.
31. Kemp BE, Pearson RB (1990) Protein kinase recognition sequence motifs. *Trends Biochem Sci* 15:342–346.